To appear in Proc. 48th IEEE CDC

Three-Dimensional Motion Coordination in a Time-Invariant Flowfield

Sonia Hernandez and Derek A. Paley

***Abstract*— Three-dimensional motion coordination in a flowfield has applications in environmental monitoring with autonomous vehicles. Motion-coordination algorithms designed using a flow-free motion model often fail to converge in even moderate flow speeds. We apply Lyapunov-based methods to design decentralized feedback laws for use in a three-dimensional, time-invariant flowfield that does not exceed the speed of each platform relative to the flow. The control laws stabilize moving formations in a dynamic model of identical particles that travel at constant speed relative to the flow. Specifically, we provide theoretically justified algorithms to stabilize parallel, helical, and circular formations in a three dimensional flowfield. In ongoing work, we seek to extend the three-dimensional motion-coordination framework to address strong and time-varying flowfields that represent more realistic environmental dynamics in the atmosphere and ocean.**

I. INTRODUCTION

Stabilization of collective motion in three dimensions using feedback control provides a robust sensing methodology for synoptic and adaptive sampling in the air [1] and sea [2]. For example, Areosonde unmanned aerial vehicles have flown into hurricanes to obtain flow data [3]. Also, autonomous underwater gliders provide a robust platform for synoptic data collection of spatiotemporal processes in the ocean [4]. In environmental monitoring applications, it is often difficult to coordinate the motion of autonomous vehicles due to external flowfields such as ocean currents and atmospheric winds. This challenge highlights the need to develop theoretically justified algorithms that stabilize three-dimensional collective motion in the presence of a flowfield [5], [6].

Previous work on collective motion in a flowfield has focused on a *planar* model of self-propelled particles [6], [7], [8]. A planar model is sufficient for stabilizing collective motion in a small-scale operating domain. However, motivated by unmanned vehicles that perform volumetric sampling—such as underwater gliders and unmanned aircraft—we are interested in studying a three-dimensional model. For constant altitude/depth surveys on scales where the curvature and/or rotation of the earth are relevant, a two-dimensional model in which particles are constrained to the surface of a sphere has been studied [9], [10]. Most of the work done in *three-dimensional* collective motion has focused on flow-free models with possibly limited communication [11], [12], [9]. We extend this work by studying collective motion in a time-invariant, three-dimensional flowfield.

S. Hernandez is a graduate student in the Department of Aerospace Engineering, University of Texas at Austin, Austin, TX 78712, USA

D. A. Paley is an Assistant Professor in the Department of Aerospace Engineering, University of Maryland, College Park, MD 20742, USA dpaley@umd.edu

This paper extends [11], [12] (also see [13]), which use geometric-control methods to provide decentralized algorithms that stabilize relative equilibria in a flow-free, three-dimensional model of self-propelled particles. Three-dimensional motion coordination using geometric control has also been studied in [14]. We follow the development in [6] and [10] (also see [15], [8]), which describe a planar framework for stabilizing collective motion in a time-invariant flow. Although we assume that all-to-all communication is available, this framework is easily extended to networks with limited communication [16].

The contributions of the paper are as follows. First, we add a time-invariant flowfield to a model courtesy of [11] of self-propelled particles that travel in three dimensions. Second, we adapt for operation in a time-invariant flowfield theoretically justified decentralized control laws that steer the particles into parallel, helical, or circular formations [12]. These formations are relative equilibria of the flow-free three-dimensional particle model [11]. We assume that the flowfield is known locally by each particle, continuously differentiable, and has magnitude everywhere less than the particle speed relative to the flow.

Studying particles that converge to helical motion under a flowfield draws particular interest because unmanned aerial vehicles in a helical formation can be used to obtain real-time hurricane data. We use numerical simulations to illustrate the application of the proposed control algorithms in circulating flows that resemble a hurricane model.

The paper is organized as follows. In Section II we describe the flow-free model of self-propelled particles in three dimensions. In Section III, we introduce the three-dimensional motion model with a time-invariant flowfield. In Section IV we provide control laws that stabilize parallel, helical, and circular formations. Section V summarizes our results and discusses future work.

II. FLOW-FREE PARTICLE MODEL

The model presented in Section III adds a three-dimensional flowfield to the flow-free, three-dimensional model introduced in [11] and further studied in [12]. We summarize the flow-free model here. It consists of N identical particles moving at unit speed (Fig. 1(a)).

The position of particle k, where $k \in \{1, \dots, N\}$, is represented by $\mathbf{r}_k \in \mathbb{R}^3$ and its velocity relative to an inertial frame $\mathcal{I}$ by $\dot{\mathbf{r}}_k$. Control $\mathbf{u}_k = [w_k \ -h_k \ q_k]^T \in \mathbb{R}^3$ steers each particle by rotating the velocity about the unit vectors of a path frame, $\mathcal{C}_k = (k, \mathbf{x}_k, \mathbf{y}_k, \mathbf{z}_k)$, where $\mathbf{x}_k, \mathbf{y}_k, \mathbf{z}_k \in \mathbb{R}^3$. $\mathcal{C}_k$ is fixed to particle k such that the unit vector $\mathbf{x}_k$ points in the direction of the velocity of particle k. ($\mathcal{C}_k$ is a right-handed

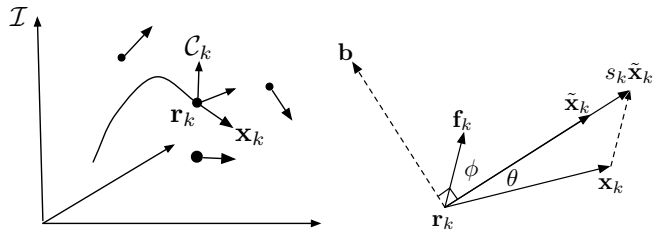

(a) Flow-free model (b) Model with flow

Fig. 1. Schematic of vectors used in the 3D motion models. (a) In the flow-free model (1), a path frame $\mathcal{C}_k$ is aligned with the velocity of particle k relative to an inertial frame $\mathcal{I}$. (b) In the model (4) with flow $\mathbf{f}$, the inertial velocity of particle k is $\mathbf{x}_k + \mathbf{f}_k$ (not used until Section III).

reference frame.) The equations of motion are [11]

$$\begin{array}{rcl} \dot{\mathbf{r}}_k &=& \mathbf{x}_k \\ \dot{\mathbf{x}}_k &=& q_k\mathbf{y}_k + h_k\mathbf{z}_k \\ \dot{\mathbf{y}}_k &=& -q_k\mathbf{x}_k + w_k\mathbf{z}_k \\ \dot{\mathbf{z}}_k &=& -h_k\mathbf{x}_k - w_k\mathbf{y}_k, \end{array} \tag{1}$$

where q_k (resp. h_k) represents the curvature control of the kth particle about the $\mathbf{y}_k$ (resp. $\mathbf{z}_k$) axis. The torsion control w_k allows the velocity of particle k to rotate about the $\mathbf{x}_k$ axis.

The dynamics in (1) represent a control system on the Lie group $SE(3)$ [11], [12] and, consequently, can be expressed in terms of the group variable

$$g_k = \left[\begin{array}{cc} R_k & \mathbf{r}_k \\ \mathbf{0} & 1 \end{array} \right] \in SE(3),$$

where $R_k = [\mathbf{x}_k \ \mathbf{y}_k \ \mathbf{z}_k]$. The dynamics (1) are equivalent to $\dot{g}_k = g_k\hat{\boldsymbol{\xi}}_k$, where $\hat{\boldsymbol{\xi}}_k \in \mathfrak{se}(3)$ is an element of the Lie algebra of $SE(3)$ given by

$$\hat{\boldsymbol{\xi}}_k = \left[\begin{array}{cc} \hat{\mathbf{u}}_k & \mathbf{e}_1 \\ \mathbf{0} & 0 \end{array} \right]$$

and $\mathbf{e}_1 = [1 \quad 0 \quad 0]^T$. $\hat{\mathbf{u}}_k$ is the 3×3 skew-symmetric matrix that represents an element of $\mathfrak{so}(3)$, the Lie Algebra of $SO(3)$.

III. PARTICLE MOTION IN A FLOWFIELD

In this section, we introduce a model of N particles traveling in a three-dimensional, time-invariant flowfield $\mathbf{f}$. The velocity of the flow at $\mathbf{r}_k$ is denoted by $\mathbf{f}_k = \mathbf{f}(\mathbf{r}_k)$. Expressed in vector components with respect to the path frame C_k, the flow is

$$\mathbf{f}_k = p_k\mathbf{x}_k + t_k\mathbf{y}_k + v_k\mathbf{z}_k, \tag{2}$$

where $p_k = \mathbf{f}_k \cdot \mathbf{x}_k$, $t_k = \mathbf{f}_k \cdot \mathbf{y}_k$, and $v_k = \mathbf{f}_k \cdot \mathbf{z}_k$. We assume that the flow is known locally by each particle, continuously differentiable, and $||\mathbf{f}_k|| < 1 \ \forall \ k$. The last assumption ensures that a particle can always make forward progress as measured from an inertial frame. The inertial velocity of particle k is the sum of its velocity relative to the flow and the velocity of the flow,

$$\dot{\mathbf{r}}_k = \mathbf{x}_k + \mathbf{f}_k = (1 + p_k)\mathbf{x}_k + t_k\mathbf{y}_k + v_k\mathbf{z}_k. \tag{3}$$

Note, the speed of particle k relative to the flow is always one.

We associate frame $\mathcal{C}_k$ with motion relative to the flowfield. In order to find a control law to stabilize a formation in a time-invariant flow, we express the dynamics (1) with $\dot{\mathbf{r}}_k$ given by (3) using a second path frame, $\mathcal{D}_k = (k, \tilde{\mathbf{x}}_k, \tilde{\mathbf{y}}_k, \tilde{\mathbf{z}}_k)$, which is aligned with the *inertial* velocity of particle k, i.e., $\tilde{\mathbf{x}}_k$ is parallel to $\dot{\mathbf{r}}_k$. (The mapping from $\mathcal{C}_k$ to $\mathcal{D}_k$ is given below). Let $s_k = ||\mathbf{x}_k + \mathbf{f}_k||$ be the inertial speed of particle k. The dynamics expressed as components in the inertial path frame are

$$\begin{array}{rcl} \dot{\mathbf{r}}_k &=& s_k\tilde{\mathbf{x}}_k \\ \dot{\tilde{\mathbf{x}}}_k &=& \tilde{q}_k\tilde{\mathbf{y}}_k + \tilde{h}_k\tilde{\mathbf{z}}_k \\ \dot{\tilde{\mathbf{y}}}_k &=& -\tilde{q}_k\tilde{\mathbf{x}}_k + \tilde{w}_k\tilde{\mathbf{z}}_k \\ \dot{\tilde{\mathbf{z}}}_k &=& -\tilde{h}_k\tilde{\mathbf{x}}_k - \tilde{w}_k\tilde{\mathbf{y}}_k, \end{array} \tag{4}$$

where $\tilde{\mathbf{u}}_k = [\tilde{w}_k \quad -\tilde{h}_k \quad \tilde{q}_k]^T$ are the steering controls relative to frame $\mathcal{D}_k$. Note that the dynamics in (4) still represent a model in SE(3), since

$$\dot{\tilde{g}}_k = \tilde{g}_k\hat{\tilde{\boldsymbol{\xi}}}_k = \left[\begin{array}{cc} \tilde{R}_k & \tilde{\mathbf{r}}_k \\ \mathbf{0} & 1 \end{array} \right] \left[\begin{array}{cc} \hat{\tilde{\mathbf{u}}}_k & s_k\mathbf{e}_1 \\ \mathbf{0} & 0 \end{array} \right], \tag{5}$$

where $\tilde{R}_k = [\tilde{\mathbf{x}}_k \quad \tilde{\mathbf{y}}_k \quad \tilde{\mathbf{z}}_k]$ and $\hat{\tilde{\mathbf{u}}} \in \mathfrak{se}(3)$. We will later make use of the fact that (4) implies

$$\dot{\tilde{\mathbf{x}}}_k = \tilde{R}_k\tilde{\mathbf{u}}_k \times \tilde{\mathbf{x}}_k. \tag{6}$$

A. Transformation between relative and inertial path frames

We use (3) and (4) to derive the relationship between frames $\mathcal{C}_k$ and $\mathcal{D}_k$. Also, since we design the steering controls $\tilde{\mathbf{u}}_k$ using (4) and the platform dynamics are presumed to obey (1), it is important for applications to find $\mathbf{u}_k$ in terms of $\tilde{\mathbf{u}}_k$ and $\mathbf{f}_k$.

We consider separately three individual cases: (i) $t_k \neq 0$ and $v_k \neq 0$; (ii) $t_k = 0$ and $v_k \neq 0$ (or $v_k = 0$ and $t_k \neq 0$); and (iii) $t_k = v_k = 0$. For each case, we provide the transformation between the C_k and D_k frames and an analytical expression for each component of $\mathbf{u}_k$ in terms of the components of $\tilde{\mathbf{u}}_k$ and $\mathbf{f}_k$.

By definition, we have

$$\tilde{\mathbf{x}}_k \quad = \quad \frac{1 + p_k}{s_k}\mathbf{x}_k + \frac{t_k}{s_k}\mathbf{y}_k + \frac{v_k}{s_k}\mathbf{z}_k. \tag{7}$$

Let θ be the angle between $\mathbf{x}_k$ and $\tilde{\mathbf{x}}_k$, such that $0 \leq \theta \leq \pi$ (see Fig. 1(b)), which implies

$$\begin{array}{rcl} \cos\theta &=& \mathbf{x}_k \cdot \tilde{\mathbf{x}}_k = \dfrac{1 + p_k}{s_k} \\ \sin\theta &=& ||\mathbf{x}_k \times \tilde{\mathbf{x}}_k|| = \dfrac{\sqrt{t_k^2 + v_k^2}}{s_k}. \end{array} \tag{8}$$

Case i: If $t_k \neq 0$ and $v_k \neq 0$, we define the unit vector

$$\mathbf{c} = \frac{\mathbf{x}_k \times \mathbf{f}_k}{||\mathbf{x}_k \times \mathbf{f}_k||} = \frac{-v_k\mathbf{y}_k + t_k\mathbf{z}_k}{(t_k^2 + v_k^2)^{1/2}}$$

to be orthogonal to the plane spanned by $\mathbf{x}_k$ and $\mathbf{f}_k$. The rotation matrix ${}^{\mathcal{D}_k}R^{\mathcal{C}_k}$ that relates frames $\mathcal{C}_k$ and $\mathcal{D}_k$ is [17]

$${}^{\mathcal{D}_k}R_k^{\mathcal{C}_k} = \left[\begin{array}{ccc} \cos\theta & c_3\sin\theta & -c_2\sin\theta \\ -c_3\sin\theta & c_2^2\mu_\theta + \cos\theta & -c_2c_3\mu_\theta \\ c_2\sin\theta & -c_2c_3\mu_\theta & c_3^2\mu_\theta + \cos\theta \end{array} \right] \tag{9}$$

where $c_2 = -(t_k^2 + v_k^2)^{-1/2} v_k$ and $c_3 = (t_k^2 + v_k^2)^{-1/2} t_k$ are the components of $\mathbf{c}$ expressed in frame $\mathcal{C}_k$, $\cos\theta$ and $\sin\theta$ are given by (8), and $\mu_\theta = 1 - \cos\theta$. Using (9), we relate the unit vectors in D_k and C_k by

$$\begin{bmatrix} \tilde{\mathbf{x}}_k^T \\ \tilde{\mathbf{y}}_k^T \\ \tilde{\mathbf{z}}_k^T \end{bmatrix} = {}^{\mathcal{D}_k}R^{\mathcal{C}_k} \begin{bmatrix} \mathbf{x}_k^T \\ \mathbf{y}_k^T \\ \mathbf{z}_k^T \end{bmatrix}. \tag{10}$$

To solve for the components of $\mathbf{u}_k$, we take the time derivative of each side of (7) and use (1) to obtain

$$\begin{aligned} \frac{d}{dt}\tilde{\mathbf{x}}_k = &\left[\frac{d}{dt}\left(\frac{1+p_k}{s_k}\right) - \frac{t_k + v_k}{s_k}\right]\mathbf{x}_k \\ &+ \left[\frac{(1+p_k)q_k - v_k w_k}{s_k} + \frac{d}{dt}\left(\frac{t_k}{s_k}\right)\right]\mathbf{y}_k \\ &+ \left[\frac{d}{dt}\left(\frac{v_k}{s_k}\right) + \frac{(1+p_k)h_k + t_k w_k}{s_k}\right]\mathbf{z}_k. \end{aligned} \tag{11}$$

We then use (10) to compare the components of (11) to the components of $\dot{\tilde{\mathbf{x}}}_k$ given in (4). The expressions for h_k, q_k, and w_k are

$$h_k = \frac{-\dot{s}_k s_k^{-1}(1+p_k) + t_k\tilde{q}_k + v_k\tilde{h}_k + \dot{p}_k - t_k q_k}{v_k} \tag{12}$$

$$\begin{aligned} q_k &= \frac{\dot{s}_k s_k^{-1} t_k + w_k v_k - \dot{t}_k}{1+p_k} \\ &+ \frac{\tilde{q}_k(s_k v_k^2 + t_k^2(1+p_k)) - \tilde{h}_k v_k t_k (s_k - (1+p_k))}{(1+p_k)(t_k^2 + v_k^2)} \end{aligned} \tag{13}$$

$$\begin{aligned} w_k &= \frac{1}{t_k}\left[\dot{s}_k s_k^{-1} v_k - h_k(1+p_k) - \dot{v}_k\right] \\ &+ \frac{\tilde{h}_k(s_k t_k^2 + v_k^2(1+p_k) - \tilde{q}_k v_k t_k (s_k - (1+p_k))}{t_k(t_k^2 + v_k^2)}. \end{aligned} \tag{14}$$

Since in this case we assumed that neither t_k nor v_k are equal to zero and $|p_k| \neq 1$, the expressions (12–14) are nonsingular. Also, the derivatives exist because $\mathbf{f}_k$ is differentiable.

Case ii: If $t_k = 0$ and $v_k \neq 0$, using (9) and (10), the relationship between $\mathcal{C}_k$ and $\mathcal{D}_k$ reduces to

$$\begin{bmatrix} \tilde{\mathbf{x}}_k^T \\ \tilde{\mathbf{z}}_k^T \end{bmatrix} = \begin{bmatrix} \cos\theta & \sin\theta \\ -\sin\theta & \cos\theta \end{bmatrix} \begin{bmatrix} \mathbf{x}_k^T \\ \mathbf{z}_k^T \end{bmatrix}. \tag{15}$$

and $\mathbf{y}_k$ and $\tilde{\mathbf{y}}_k$ are equal.

To find $\mathbf{u}_k$ in terms of $\tilde{\mathbf{u}}_k$, we use (15) to compare the components of (11) to the components of $\dot{\tilde{\mathbf{x}}}_k$ in (4). The expressions for h_k and q_k are

$$h_k = \tilde{h}_k + \frac{s_k}{v_k}\frac{d}{dt}\left(\frac{1+p_k}{s_k}\right) \tag{16}$$

$$q_k = \frac{s_k\tilde{q}_k + v_k w_k}{1+p_k}. \tag{17}$$

Equations (16)–(17) are nonsingular since $v_k \neq 0$, $|p_k| \neq 1$, and $s_k > 0$ by assumption. To find w_k, we use (4) and the time derivative of $\tilde{\mathbf{z}}_k$ to obtain

$$w_k = v_k^2\left(\tilde{h}_k + h_k\right)\frac{1}{s_k v_k^2}. \tag{18}$$

Equation (18) is nonsingular, since we have assumed that $v_k \neq 0$. The case when $v_k = 0$ and $t_k \neq 0$ follows similarly.

Case iii: If $t_k = v_k = 0$, then frames $\mathcal{C}_k$ and $\mathcal{D}_k$ are equal, since $\mathbf{x}_k$ and $\tilde{\mathbf{x}}_k$ are parallel. ($\mathbf{x}_k$ and $\tilde{\mathbf{x}}_k$ cannot be antiparallel since we have assumed particle k always makes forward progress relative to the flow.) In this case, $\mathbf{u}_k = \tilde{\mathbf{u}}_k$.

B. Inertial speed in a 3D flowfield

Unlike in the flow-free model (1), the inertial speed of particle k in model (4) is not constant—it depends on the flow and the direction of motion. Using (7), the inertial speed of particle k is

$$s_k = ||s_k\tilde{\mathbf{x}}_k|| = \sqrt{(1+p_k)^2 + t_k^2 + v_k^2} > 0,$$

where p_k, t_k, and v_k are components of $\mathbf{f}_k$ in frame $\mathcal{C}_k$. In order to integrate (4), we calculate an expression for s_k in terms of the components of $\mathbf{f}_k$ in frame $\mathcal{D}_k$.

Let $\mathbf{b}$ be a unit vector orthogonal to $\tilde{\mathbf{x}}_k$ in the plane spanned by $\mathbf{x}_k$ and $\mathbf{f}_k$ as shown in Fig. 1(b). Let ϕ denote the angle between $\tilde{\mathbf{x}}_k$ and $\mathbf{f}_k$. We have

$$\begin{aligned} \cos\phi &= \frac{\mathbf{f}_k \cdot \tilde{\mathbf{x}}_k}{\|\mathbf{f}_k\|} \\ \sin\phi &= \frac{\mathbf{f}_k \cdot \mathbf{b}}{\|\mathbf{f}_k\|}. \end{aligned}$$

It is also true that

$$\frac{\|\tilde{\mathbf{x}}_k \times \mathbf{f}_k\|}{\|\mathbf{f}_k\|} = |\sin\phi|,$$

which implies

$$\|\tilde{\mathbf{x}}_k \times \mathbf{f}_k\| = |\mathbf{f}_k \cdot \mathbf{b}|.$$

Also, the fact that $\mathbf{x}_k = (\mathbf{x}_k \cdot \tilde{\mathbf{x}}_k)\tilde{\mathbf{x}}_k + (\mathbf{x}_k \cdot \mathbf{b})\mathbf{b}$ implies

$$\|\mathbf{x}_k\|^2 = (\mathbf{x}_k \cdot \tilde{\mathbf{x}}_k)^2 + (\mathbf{x}_k \cdot \mathbf{b})^2 = 1.$$

Dotting both sides of the speed equation $s_k\tilde{\mathbf{x}}_k = \mathbf{x}_k + \mathbf{f}_k$ first by $\tilde{\mathbf{x}}_k$ and then by $\mathbf{b}$ yields

$$\begin{aligned} s_k &= \mathbf{x}_k \cdot \tilde{\mathbf{x}}_k + \mathbf{f}_k \cdot \tilde{\mathbf{x}}_k \\ 0 &= \mathbf{x}_k \cdot \mathbf{b} + \mathbf{f}_k \cdot \mathbf{b}. \end{aligned}$$

We have

$$\begin{aligned} s_k &= \pm\sqrt{1 - (\mathbf{x}_k \cdot \mathbf{b})^2} + \mathbf{f}_k \cdot \tilde{\mathbf{x}}_k \\ &= \pm\sqrt{1 - (\mathbf{f}_k \cdot \mathbf{b})^2} + \mathbf{f}_k \cdot \tilde{\mathbf{x}}_k \\ &= \pm\sqrt{1 - \|\tilde{\mathbf{x}}_k \times \mathbf{f}_k\|^2} + \mathbf{f}_k \cdot \tilde{\mathbf{x}}_k \end{aligned} \tag{19}$$

Of the two solutions for s_k provided by (19) only the positive root yields $s_k > 0$. The fact that the negative root leads to a negative solution for s_k can be proven by contradiction. Assume that $s_k = -\sqrt{1 - \|\tilde{\mathbf{x}}_k \times \mathbf{f}_k\|^2} + \mathbf{f}_k \cdot \tilde{\mathbf{x}}_k > 0$. Observe that

$$\|\tilde{\mathbf{x}}_k \times \mathbf{f}_k\|^2 + (\mathbf{f}_k \cdot \tilde{\mathbf{x}}_k)^2 = \|\mathbf{f}_k\| < 1.$$

Then we have

$$s_k < -\sqrt{1 - (1 - (\mathbf{f}_k \cdot \tilde{\mathbf{x}}_k)^2)} + \mathbf{f}_k \cdot \tilde{\mathbf{x}}_k = -|\mathbf{f}_k \cdot \tilde{\mathbf{x}}_k| + \mathbf{f}_k \cdot \tilde{\mathbf{x}}_k \leq 0,$$

which is a contradiction. Therefore, the inertial speed of particle k in flow $\mathbf{f}$ is

$$s_k = \sqrt{1 - \|\tilde{\mathbf{x}}_k \times \mathbf{f}_k\|^2} + \mathbf{f}_k \cdot \tilde{\mathbf{x}}_k. \tag{20}$$

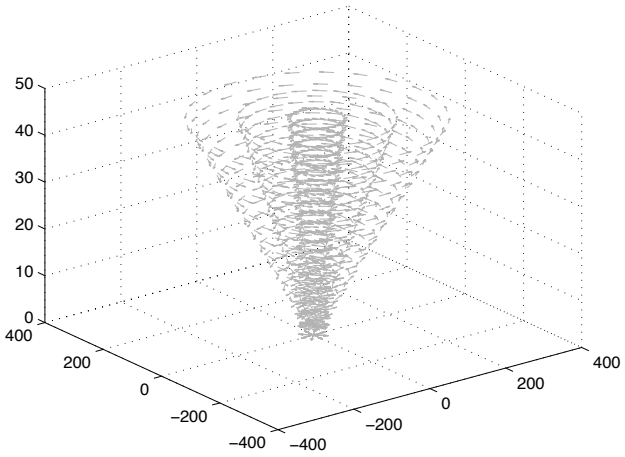

Fig. 2. Simple hurricane model with uniform flowspeed. The flowfield is circular with increasing radius and height.

Note, (20) is used to integrate (4) and only requires knowledge of $\mathbf{f}_k(t)$ expressed in $\mathcal{D}_k$. However, to compute $\mathbf{u}_k$ from $\tilde{\mathbf{u}}_k$, we need to know $\mathbf{f}_k(t)$ in $\mathcal{C}_k$.

IV. LYAPUNOV-BASED CONTROL DESIGN

In this section, we derive decentralized control laws that stabilize parallel, helical, and circular formations in a time-invariant flowfield, after [11], [12]. These formations are relative equilibria of the flow-free particle model [11], which means that they are steady motions that preserve—in the absence of flow—the relative positions and relative orientations of the path frames $\mathcal{C}_1, \ldots, \mathcal{C}_N$. Decentralized controls to stabilize relative equilibria in the flow-free model are provided in [12].

The design of a decentralized control law that stabilizes straight lines or helical motion uses the concept of *twist* [12], which is related to screw motion [17]. Following [12] we use the operator $\vee$ to find a 6-dimensional vector which parametrizes a twist of the matrix $\hat{\tilde{\boldsymbol{\xi}}}_k$, given in (5) [17],

$$\tilde{\boldsymbol{\xi}}_k = \hat{\tilde{\boldsymbol{\xi}}}_k^{\vee} = \begin{bmatrix} \hat{\tilde{\mathbf{u}}}_k & s_k\mathbf{e}_1 \\ \mathbf{0} & 0 \end{bmatrix}^{\vee} = \begin{bmatrix} s_k\mathbf{e}_1 \\ \tilde{\mathbf{u}}_k \end{bmatrix} \in \mathbb{R}^6.$$

$\tilde{\boldsymbol{\xi}}_k$ is expressed in the path frame $\mathcal{D}_k$. To map the twist $\tilde{\boldsymbol{\xi}}_k$ to an inertial frame, we use the adjoint transformation [17],

$$Ad_{g_k} = \begin{bmatrix} \tilde{R}_k & \tilde{\mathbf{r}}_k\tilde{R}_k \\ 0 & \tilde{R}_k \end{bmatrix},$$

which yields[1]:

$$\tilde{\boldsymbol{\xi}}_k^a = Ad_{g_k}\tilde{\boldsymbol{\xi}}_k = \begin{bmatrix} s_k\tilde{\mathbf{x}}_k + \tilde{\mathbf{r}}_k \times \tilde{R}_k\tilde{\mathbf{u}}_k \\ \tilde{R}_k\tilde{\mathbf{u}}_k \end{bmatrix}. \qquad (21)$$

$\tilde{\boldsymbol{\xi}}_k^a$ plays the role of a *consensus* variable the sequel [12].

[1]Following the notation in [12], the superscript a indicates that the vector components are expressed in a fixed (inertial) reference frame.

A. Stabilization of Parallel Formations

A parallel formation is a steady motion in which all of the particles travel in straight, parallel lines. When the particles travel in a parallel formation, (21) reduces to

$$\boldsymbol{\xi}_k^a = \begin{bmatrix} s_k\tilde{\mathbf{x}}_k \\ \mathbf{0} \end{bmatrix}.$$

Lemma 1: Let $\mathbf{f}_k = \mathbf{f}(\mathbf{r}_k)$ be a three-dimensional, time-invariant flowfield with $\|\mathbf{f}_k\| < 1$. The control $\tilde{\mathbf{u}}_k = \mathbf{0}$ steers particle k in model (4) in a straight line such that $\tilde{\mathbf{x}}_k$ is fixed, i.e., $\dot{\tilde{\mathbf{x}}}_k = 0$. A parallel formation is characterized by the condition $\tilde{\mathbf{x}}_k = \tilde{\mathbf{x}}_j$ for all pairs $j, k \in \{1, ..., N\}$ [12].

Following [12], we choose a Lyapunov function of the form[2]

$$S(\tilde{\mathbf{x}}) = \frac{N}{2}\left(1 - \langle \tilde{\mathbf{x}}_{av}, \tilde{\mathbf{x}}_{av} \rangle\right), \qquad (22)$$

where $\tilde{\mathbf{x}}_{av} = \frac{1}{N}\sum_{j=1}^{N} \tilde{\mathbf{x}}_j$. The control law

$$\tilde{\mathbf{u}}_k = \tilde{R}_k^T(\tilde{\mathbf{x}}_k \times \tilde{\mathbf{x}}_{av}) \qquad (23)$$

ensures that the time derivative of S is non-increasing. Using (6), we have

$$\begin{aligned} \dot{S} &= -\sum_{j=1}^{N} \langle \tilde{\mathbf{x}}_{av}, \dot{\tilde{\mathbf{x}}}_j \rangle = -\sum_{j=1}^{N} \langle \tilde{\mathbf{x}}_{av}, \tilde{\mathbf{x}}_j \times \tilde{\mathbf{x}}_{av} \times \tilde{\mathbf{x}}_j \rangle \\ &= -\sum_{j=1}^{N} ||\tilde{\mathbf{x}}_k \times \tilde{\mathbf{x}}_{av}|| \leq 0. \end{aligned}$$

The following result extends [12, Theorem 1] to motion in a time-invariant flowfield.

Theorem 1: Let $\mathbf{f}_k = \mathbf{f}(\mathbf{r}_k)$ be a three-dimensional time-invariant flowfield with $||\mathbf{f}_k|| < 1$. All solutions of model (4), where the control $\tilde{\mathbf{u}}_k$ is given (23) and the speed s_k by (20), converge to the set $\{\dot{S} = 0\}$, where S is defined in (22). This set consists of parallel, balanced, and anti-parallel formations [12]. The set of parallel formations, with direction of motion determined by the initial conditions, is asymptotically stable. Every other positive limit set is unstable [12].

Theorem 1 provides a decentralized algorithm to stabilize a parallel formation in a three-dimensional flowfield. Fig. 2 shows a simple, hurricane-inspired flowfield, which is circular with increasing radius and height, i.e., it produces a cone shape. Fig. 3 depicts a parallel formation stabilized in the conical flowfield by control (23).

B. Stabilization of Circular and Helical Formations

In a helical formation, all of the particles converge to circular helices with the same axis of rotation, radius of rotation, and pitch (ratio of translational to rotational motion).

Following [12], we define the consensus variable

$$\tilde{\mathbf{v}}_k^a = \tilde{\mathbf{x}}_k + \tilde{\mathbf{r}}_k \times \boldsymbol{\omega}_0. \qquad (24)$$

[2]We drop the subscript to represent an $3N \times 1$ matrix, i.e., $\tilde{\mathbf{v}}^a = [(\tilde{\mathbf{v}}_1^a)^T, \ldots, (\tilde{\mathbf{v}}_N^a)^T]^T$.

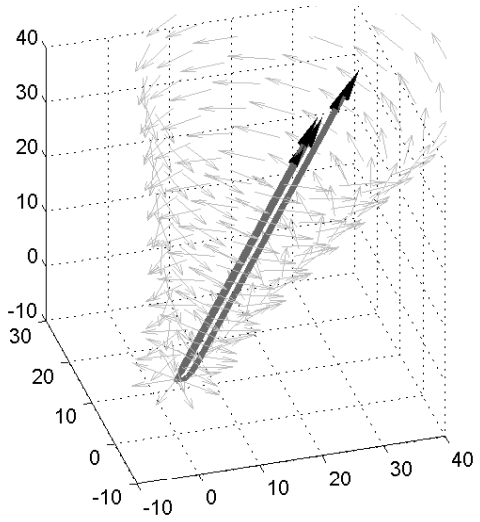

Fig. 3. Stabilization of particle model (4) to parallel motion in a time-invariant flowfield using control (23) with $N = 5$.

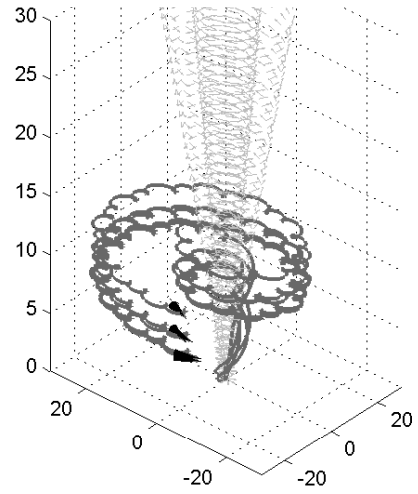

Fig. 4. The control used in [12] is implemented in the dynamics with flow in (4) with $N = 5$ particles. The particles do not converge to a helical formation.

Lemma 2: Let $\mathbf{f}_k = \mathbf{f}(\mathbf{r}_k)$ be a three-dimensional, time-invariant flowfield with $\|\mathbf{f}_k\| < 1$. The control $\tilde{\mathbf{u}}_k = \tilde{R}_k^T s_k \boldsymbol{\omega}_0$ steers particle k in model (4) around a helix such that $\tilde{\mathbf{v}}_k^a$ is fixed, i.e., $\dot{\tilde{\mathbf{v}}}_k^a = 0$, where $\tilde{\mathbf{v}}_k^a$ is defined in (24). A helical formation of N particles is characterized by the condition $\tilde{\mathbf{v}}_k^a = \tilde{\mathbf{v}}_j^a$ for all pairs j, $k \in \{1, ..., N\}$, with axis of rotation parallel to $\boldsymbol{\omega}_0$ and radius $\|\boldsymbol{\omega}_0\|^{-1}$ [12].

Now, as in [12], using the quadratic potential

$$Q(\tilde{\mathbf{v}}^a) = \frac{1}{2} \sum_{j=1}^{N} ||\tilde{\mathbf{v}}_j^a - \tilde{\mathbf{v}}_{av}^a||^2, \tag{25}$$

where $\tilde{\mathbf{v}}_{av}^a = \frac{1}{N} \sum_{j=1}^{N} \tilde{\mathbf{v}}_j^a$, yields

$$\begin{aligned} \dot{Q} &= \sum_{j=1}^{N} \langle \tilde{\mathbf{v}}_j^a - \tilde{\mathbf{v}}_{av}^a, \dot{\tilde{\mathbf{x}}}_j + \dot{\tilde{\mathbf{r}}}_j \times \boldsymbol{\omega}_0 \rangle \\ &= \sum_{j=1}^{N} \langle \tilde{\mathbf{v}}_j^a - \tilde{\mathbf{v}}_{av}^a, \tilde{\mathbf{x}}_j \times (s_j \boldsymbol{\omega}_0 - \tilde{R}_j \tilde{\mathbf{u}}_j) \rangle. \end{aligned}$$

Choosing

$$\tilde{\mathbf{u}}_k = \tilde{R}_k^T (s_k \boldsymbol{\omega}_0 + (\tilde{\mathbf{v}}_k - \tilde{\mathbf{v}}_{av}) \times \tilde{\mathbf{x}}_k), \tag{26}$$

results in

$$\dot{Q} = -\sum_{j=1}^{N} ||(\tilde{\mathbf{v}}_j^a - \tilde{\mathbf{v}}_{av}^a) \times \tilde{\mathbf{x}}_k||^2 \leq 0.$$

The following result extends [12, Theorem 2] to motion in a time-invariant flowfield.

Theorem 2: Let $\mathbf{f}_k = \mathbf{f}(\mathbf{r}_k)$ be a three-dimensional time-invariant flowfield with $\|\mathbf{f}_k\| < 1$. All solutions of model (4), where the control $\tilde{\mathbf{u}}_k$ is given by (26), the speed s_k by (20), and $\|\boldsymbol{\omega}_0\| \neq 0$, converge to the set $\{\dot{Q} = 0\}$, where Q is defined in (25). The set of helical formations with axis of rotation parallel to $\boldsymbol{\omega}_0$, radius $\|\boldsymbol{\omega}_0\|^{-1}$, and pitch determined by the initial conditions is asymptotically stable.

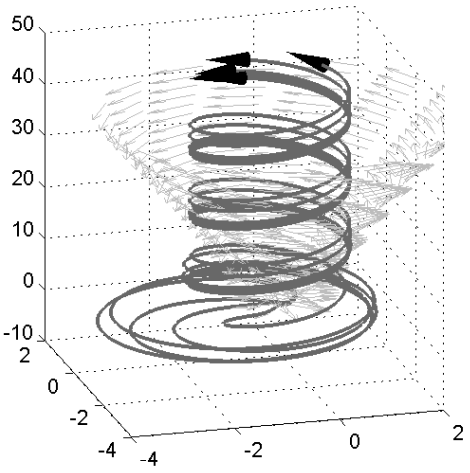

Fig. 5. Stabilization of helical motion in a simple hurricane model using the control (23) with $N = 5$ and $\boldsymbol{\omega}_0 = [0\ 0\ 1]^T$.

Theorem 2 provides a method to stabilize a helical formation in a three-dimensional time-invariant flowfield. We provide numerical simulations using the conical flowfield shown in Fig. 2. Fig. 4 shows flow-induced instability of the helical control designed using the flow-free model (1). Fig. 5 depicts a helical formation stabilized using control (26) in the conical flowfield.

A circular formation is a helical formation with zero pitch. The pitch of a helical formation stabilized by control (26) is determined by the initial conditions. To isolate helical formations with pitch $\alpha \in [0, 1)$ we use the following method adapted from [12].

Consider the composite potential [12]

$$V(\tilde{\mathbf{v}}^a) = Q(\tilde{\mathbf{v}}^a) + (N/2)\beta^2, \tag{27}$$

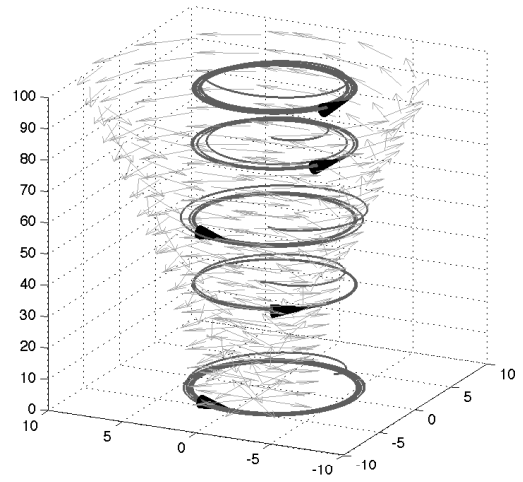

Fig. 6. Stabilization of circular motion in a simple motion hurricane model using control (29) with $\alpha = 0$, $N = 5$, and $\boldsymbol{\omega}_0 = [0\ 0\ 2]^T$.

where $Q(\tilde{\mathbf{v}}^a)$ is given by (25) and

$$\beta = \frac{\langle \boldsymbol{\omega}_0, \tilde{\mathbf{x}}_{av} \rangle}{\|\boldsymbol{\omega}_0\|} - \alpha,\ \alpha \in [0, 1). \tag{28}$$

Using the fact that $\langle \boldsymbol{\omega}_0, \boldsymbol{\omega}_0 \times \tilde{\mathbf{x}}_k \rangle = 0$, we have

$$\dot{V} = \sum_{j=1} \langle \tilde{\mathbf{v}}_j^a - \tilde{\mathbf{v}}_{av}^a + \beta \frac{\boldsymbol{\omega}_0}{\|\boldsymbol{\omega}_0\|}, (\tilde{R}_j \tilde{\mathbf{u}}_j - s_j \boldsymbol{\omega}_0) \times \tilde{\mathbf{x}}_j \rangle.$$

We ensure $\dot{V} \leq 0$ by choosing the control

$$\tilde{\mathbf{u}}_k = \tilde{R}_k^T (s_k \boldsymbol{\omega}_0 + (\tilde{\mathbf{v}}_k - \tilde{\mathbf{v}}_{av} + \beta \frac{\boldsymbol{\omega}_0}{\|\boldsymbol{\omega}_0\|}) \times \tilde{\mathbf{x}}_k). \tag{29}$$

The following result extends [12, Theorem 3] to motion in a time-invariant flowfield.

Corollary 1: Let $\mathbf{f}_k = \mathbf{f}(\mathbf{r}_k)$ be a three-dimensional time-invariant flowfield with $||\mathbf{f}_k|| < 1$. All solutions of model (4), where the control $\tilde{\mathbf{u}}_k$ is given by (29), the speed s_k by (20), β by (28), and $\|\boldsymbol{\omega}_0\| \neq 0$, converge to the set $\{\dot{V} = 0\}$, where V is defined in (27). The set of helical formations with axis of rotation parallel to $\boldsymbol{\omega}_0$, radius $\|\boldsymbol{\omega}_0\|^{-1}$, and pitch α is asymptotically stable.

Corollary 1 provides an algorithm to isolate a set of helical formations with prescribed pitch α. In particular, when $\alpha = 0$, control (29) stabilizes a set of circular formations. This is simulated in Fig. 6 in a time-invariant flowfield.

V. CONCLUSION

This paper provides decentralized controls to stabilize three-dimensional collective motion of autonomous vehicles that are subject to a time-invariant flowfield. These controls are of particular interest because they can be used to coordinate unmanned sensor platforms, such as hurricane-observation aircraft and underwater vehicles. Specifically, we provide theoretically justified algorithms that stabilize parallel, helical, and circular formations. In ongoing work we study time-varying flowfields that exceed the particle speed relative to the flow and which represent more realistic environmental dynamics in the atmosphere and ocean.

REFERENCES

[1] R. W. Beard, T. W. McLain, D. B. Nelson, D. Kingston, and D. Johanson. Decentralized cooperative aerial surveillance using fixed-wing miniature UAVs. *Proc. IEEE*, 94(7):1306–1324, 2006.

[2] N. E. Leonard, D. A. Paley, F. Lekien, R. Sepulchre, D. M. Fratantoni, and R. E. Davis. Collective motion, sensor networks and ocean sampling. *Proc. IEEE*, 95(1):48–74, 2007.

[3] G. J. Holland, P. J. Webster, J. A. Curry, G. Tyrell, D. Gauntlett, G. Brett, J. Becker, R. Hoag, and W. Vaglienti. The Aerosonde robotic aircraft: A new paradigm for environmental observations. *Bull. American Meteorological Society*, 82(5):889–901, 2001.

[4] R. E. Davis, C. E. Eriksen, and C. P. Jones. Autonomous buoyancy-driven underwater gliders. In G. Griffiths, editor, *The Technology and Applications of Autonomous Underwater Vehicles*, chapter 3, pages 37–58. Taylor and Francis, 2002.

[5] J. Elston and E. Frew. Unmanned aircraft guidance for penetration of pre-tornadic storms. In *Proc. AIAA Guidance, Navigation and Control Conf. and Exhibit (electronic)*, number AIAA-2008-6513, Honolulu, Hawaii, 2008. (16 pages).

[6] D. A. Paley and C. Peterson. Stabilization of collective motion in a time-invariant flowfield. *J. Guidance, Control, and Dynamics*, 32(3):771–779, 2009.

[7] D. J. Klein and K. A. Morgansen. Controlled collective motion for trajectory tracking. In *Proc. 2006 American Control Conf.*, pages 5269–5275, Minneapolis, Minnesota, June 2006.

[8] D. A. Paley. Cooperative Control of an Autonomous Sampling Network in an External Flow Field. In *Proc. 47th IEEE Conf. Decision and Control*, pages 3095–3100, Cancun, Mexico, December 2008.

[9] D. A. Paley. Stabilization of Collective Motion on a Sphere. *Automatica*, 45(1):212–216, 2009.

[10] S. Hernandez and D. A. Paley. Stabilization of collective motion in a time-invariant flow field on a rotating sphere. In *Proc. American Control Conf.*, pages 623–628, St. Louis, Missouri, June 2009.

[11] E. W. Justh and P. S. Krishnaprasad. Natural frames and interacting particles in three dimensions. In *Proc. Joint 44th IEEE Conf. Decision and Control and European Control Conf.*, pages 2841–2846, Seville, Spain, December 2005.

[12] L. Scardovi, N. Leonard, and R. Sepulchre. Stabilization of three-dimensional collective motion. *Communication in Information and Systems*, Brockett Legacy issue, accepted. (Preprint: arXiv: 0806.3442).

[13] L. Scardovi, N. E. Leonard, and R. Sepulchre. Stabilization of collective motion in three dimensions: A consensus approach. In *Proc. 46th IEEE Conf. Decision and Control*, pages 2931–2936, New Orleans, Louisiana, December 2007.

[14] R. Fierro, C. Belta, J. P. Desai, and V. Kumar. On controlling aircraft formations. In *Proc. IEEE Conf. Decision and Control*, volume 2, pages 1065–1070, Orlando, December 2001.

[15] D. A. Paley. Stabilization of Collective Motion in a Uniform and Constant Flow Field. In *Proc. AIAA Guidance, Navigation and Control Conf. and Exhibit*, number AIAA-2008-7173, Honolulu, Hawaii, August 2008. (8 pages).

[16] R. Sepulchre, D. A. Paley, and N. E. Leonard. . *IEEE Trans. Automatic Control*, 53(3):706–719, 2008.

[17] R. Murray, Z. Li, and S. Sastry. *A Mathematical Introduction to Robotic Manipulation*. CRC Press, 1994.